Phase transitions of the anisotropic Ashkin-Teller model on a family of diamond-type hierarchical lattices

Jian-Xin Le[2,3,*] and Z. R. Yang[1,2]
[1]*CCAST (World Laboratory), P. O. Box 8730, Beijing 100080, China*
[2]*Department of Physics and Institute of Theoretical Physics, Beijing Normal University, Beijing 100875, China*
[3]*Department of Physics, Jiangxi Normal University, Nanchang 330027, China*

(Received 2 June 2003; published 17 December 2003)

The phase transitions of the anisotropic Ashkin-Teller model on a family of diamond-type hierarchical lattices is studied by means of the transfer-matrix method and the real-space renormalization-group transformation. We find that the phase diagram, for the ferromagnetic case, consists of five phases, i.e., the fully disordered paramagnetic phase *P*, the fully ordered ferromagnetic phase *F*, and three partially ordered ferromagnetic phases F_s, F_σ, and $F_{s\sigma}$, as well as ten nontrivial fixed points. The correlation length critical exponents and the crossover exponents are also calculated. In addition, we also investigate the variations of the critical exponents with the fractal dimension d_f, the number of branches *m*, and the number of bonds per branch *b* of the generator of the family of diamond-type hierarchical lattices. Finally we give a brief discussion about universality.

DOI: 10.1103/PhysRevE.68.066105 PACS number(s): 05.50.+q, 75.10.Hk, 64.60.Ak

I. INTRODUCTION

The Ashkin-Teller (AT) model [1] is a generalization of the Ising model to a four-component system. In this case, each site of a lattice is occupied by one of the four different kinds of atoms *A*, *B*, *C*, or *D*. Two nearest-neighbor atoms interact with an energy; ϵ_0 for $A-A$, $B-B$, $C-C$, $D-D$; ϵ_1 for $A-B$, $C-D$; ϵ_2 for $A-C$, $B-D$; and ϵ_3 for $A-D$, $B-C$. Fan [2] associated each lattice site *i* with two spin variables s_i and σ_i and represented the four states *A*, *B*, *C*, and *D* by the spin configurations (s_i,σ_i): $(+,+)$, $(+,-)$, $(-,+)$, and $(-,-)$, correspondingly. Thus the AT model can be expressed in terms of the Ising spins, the Hamiltonian for the magnetic system being

$$H=-\sum_{\langle ij\rangle}(J_s s_i s_j+J_\sigma\sigma_i\sigma_j+J_4 s_i\sigma_i s_j\sigma_j+J_0), \qquad (1)$$

where the sum $\Sigma_{\langle ij\rangle}$ runs over all the nearest-neighbor pairs of spins. In this sense, the AT model may be considered to be two superposed Ising models described by two spin variables s_i and σ_i, respectively. J_s and J_σ represent the two-spin nearest-neighbor interaction strength within the two Ising models, respectively. In addition, the different Ising models are coupled by a four-spin interaction with strength J_4. If $J_s=J_\sigma$, this corresponds to the isotropic case where the two Ising systems are identical with each other.

Wegner [3] has shown that the AT model is equivalent to a staggered eight-vertex model, which remains unsolved exactly. In two dimensions, the phase diagram for the isotropic AT model has been studied extensively by means of experimental technique [4], Monte Carlo simulations [5–8], and various theoretical methods [9–13]. It can be found that the phase diagram has a very rich structure, containing one paramagnetic phase, one ferromagnetic phase, and one partially ordered phase, which are separated by two Ising-type critical lines and a critical line of continuously varying exponents known exactly [14]. Ditzian and his collaborators [15] found that for the isotropic AT model, the phase diagram for the three-dimensional system is much richer than, and quite different from, that in two dimensions. There appear some first-order phase transitions and continuous phase transitions, even an XY-like transition and a Heisenberg-like multicritical point. With respect to the anisotropic AT model, in which the two Ising systems are not identical with each other, the phase diagram, however, is not so clear. Wu and Lin [16] have employed exact duality relations to determine the phase diagram for the anisotropic AT model on the square lattice. In addition, some approaches, such as renormalization-group transforamtion [17], finite-size-scaling [18], mean-field approximation, and Monte Carlo simulations [19], have been applied to the investigations of the phase diagram for the anisotropic AT model as well.

So far, most of the research on the AT model has been focused on the translational symmetry lattices, i.e., Bravais lattices, whereas much less attention has been paid to the study of this model on the fractal lattices, e.g., the hierarchical lattices. As noted by Berker and Ostlund [20], certain renormalization-group transformations, which are only approximate on the translational symmetry lattices, become exact on the hierarchical lattices. On the other hand, the hierarchical lattices are highly inhomogeneous [21], and they may provide insights into other low-symmetry problems such as random magnets, surfaces, etc. Therefore, much work on the hierarchical lattices has been motivated recently [22–25]. It is worthwhile to mention that Bezerra *et al.* [26] have investigated the anisotropic AT model on a kind of self-dual hierarchical lattice and obtained the phase diagram as well as the critical exponents.

In this paper, using the transfer-matrix method and the real-space renormalization-group transformation, we study the phase transitions of the anisotropic Ashkin-Teller model

*Electronic address: jianxinle@yahoo.com

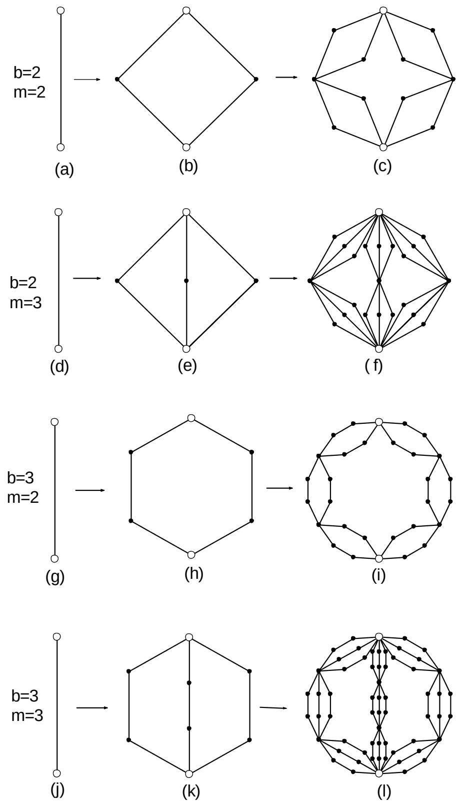

FIG. 1. First two stages of the constructions of a few members of the family of the diamond-type hierarchical lattices.

on a family of diamond-type hierarchical lattices. It can be found that the phase diagram, for the ferromagnetic case, consists of five phases, i.e., the fully disordered paramagnetic phase P, the fully ordered ferromagnetic phase F, and three partially ordered ferromagnetic phases F_s, F_σ, and $F_{s\sigma}$, as well as ten nontrivial fixed points. The correlation length critical exponents and the crossover exponents are also calculated. In addition, we also investigate the variations of the critical exponents with the fractal dimension and other geometrical parameters of the lattices. In the following section, the recursion relations of the renormalization-group transformation are obtained. In Sec. III, the fixed points and the phase diagrams are presented. The critical exponents are calculated in Sec. IV. Finally, we give a brief discussion and conclusion in Sec. V.

II. THE RECURSION RELATIONS OF RENORMALIZATION-GROUP TRANSFORMATION

As we know, the hierarchical lattices can be constructed in an iterative manner. Herein we shall restrict ourselves to a family of diamond-type hierarchical lattices [27,28], the constructions of which can be realized through iterative decoration of a two-point bond by a generator, which has two vertices joined by m branches of b bonds. Figure 1 shows the constructions of a few members of the family. For these structures, one can employ a well-defined fractal dimension d_f to describe their geometrical features, i.e.,

$$d_f = \frac{\ln(mb)}{\ln b} = 1 + \frac{\ln m}{\ln b}, \tag{2}$$

where m and b denote the number of branches, and the number of bonds per branch of the generator of the hierarchical lattice, respectively.

For the reasons that the term $\Sigma_{\langle ij\rangle} J_0$ in expression (1) is irrelevant to the spins s and σ, and only contributes to the nonsingular part of the free energy, one does not need to consider it in the process of the renormalization-group transformation. Thus, the effective Hamiltonian $\mathcal{H}$ for the anisotropic AT model can be expressed as

$$\mathcal{H} = \sum_{\langle ij\rangle} (K_s s_i s_j + K_\sigma \sigma_i \sigma_j + K_4 s_i \sigma_i s_j \sigma_j), \tag{3}$$

where $K_s = \beta J_s$, $K_\sigma = \beta J_\sigma$, $K_4 = \beta J_4$, $\beta = 1/(k_B T)$, k_B is the Boltzmann's constant, T is the absolute temperature, and the sum $\Sigma_{\langle ij\rangle}$ runs over all the nearest-neighbor pairs of spins. The partition function is written as

$$Z(K_s, K_\sigma, K_4) = \sum_{\{s,\sigma\}} \exp(\mathcal{H}), \tag{4}$$

where the summation $\Sigma_{\{s,\sigma\}}$ is over the values $+1$ and -1 of all site spins on the lattice.

In this case, the renormalization-group transformation requires

$$A \exp(\mathcal{H}'_{1,2}) = \sum_{\{s_3,\sigma_3\}} \sum_{\{s_4,\sigma_4\}} \cdots \times \sum_{\{s_{m(b-1)+2}, \sigma_{m(b-1)+2}\}} \exp(\mathcal{H}_{1,2,\ldots,m(b-1)+2}), \tag{5}$$

where $\mathcal{H}_{1,2,\ldots,m(b-1)+2}$ denotes the effective Hamiltonian of the generator of the diamond-type hierarchical lattice, $\mathcal{H}'_{1,2}$ represents the effective Hamiltonian of the two-vertex bond after the renormalization-group transformation is performed, the subscripts 1 and 2 stand for the two vertices of the generator, the others $3,4,\ldots,m(b-1)+2$ are the internal sites of the generator, $m(b-1)$ and $m(b-1)+2$ are the number of the internal sites, and the number of the total sites of the generator, respectively, A is an additive constant produced after the transformation, and the summations are over all values of all internal site spins of the generator of the diamond-type hierarchical lattice.

By means of the transfer-matrix method, we can decimate all internal site spins on the hierarchical lattice. The elements of the transfer-matrix Q are defined as

$$\langle \sigma_i, s_i | Q | s_j, \sigma_j \rangle = \exp(K_s s_i s_j + K_\sigma \sigma_i \sigma_j + K_4 s_i \sigma_i s_j \sigma_j). \tag{6}$$

Thus Eq. (5) becomes

$$A \langle \sigma_1, s_1 | Q' | s_2, \sigma_2 \rangle = (\langle \sigma_1, s_1 | Q^b | s_2, \sigma_2 \rangle)^m. \tag{7}$$

From Eq. (7), one can get that

$$A_i \exp(K_s^{(i-1)}+K_\sigma^{(i-1)}+K_4^{(i-1)}) = \frac{1}{4^m}(q_1^b+q_2^b+q_3^b+q_4^b)^m, \tag{8}$$

$$A_i \exp(K_s^{(i-1)}-K_\sigma^{(i-1)}-K_4^{(i-1)}) = \frac{1}{4^m}(q_1^b-q_2^b-q_3^b+q_4^b)^m, \tag{9}$$

$$A_i \exp(-K_s^{(i-1)}+K_\sigma^{(i-1)}-K_4^{(i-1)}) = \frac{1}{4^m}(-q_1^b+q_2^b-q_3^b+q_4^b)^m, \tag{10}$$

and

$$A_i \exp(-K_s^{(i-1)}-K_\sigma^{(i-1)}+K_4^{(i-1)}) = \frac{1}{4^m}(-q_1^b-q_2^b+q_3^b+q_4^b)^m, \tag{11}$$

where

$$\begin{aligned} q_1 = {}& \exp(K_s^{(i)}+K_\sigma^{(i)}+K_4^{(i)}) + \exp(K_s^{(i)}-K_\sigma^{(i)}-K_4^{(i)}) \\ & -\exp(-K_s^{(i)}+K_\sigma^{(i)}-K_4^{(i)}) \\ & -\exp(-K_s^{(i)}-K_\sigma^{(i)}+K_4^{(i)}), \end{aligned} \tag{12}$$

$$\begin{aligned} q_2 = {}& \exp(K_s^{(i)}+K_\sigma^{(i)}+K_4^{(i)}) - \exp(K_s^{(i)}-K_\sigma^{(i)}-K_4^{(i)}) \\ & +\exp(-K_s^{(i)}+K_\sigma^{(i)}-K_4^{(i)}) \\ & -\exp(-K_s^{(i)}-K_\sigma^{(i)}+K_4^{(i)}), \end{aligned} \tag{13}$$

$$\begin{aligned} q_3 = {}& \exp(K_s^{(i)}+K_\sigma^{(i)}+K_4^{(i)}) - \exp(K_s^{(i)}-K_\sigma^{(i)}-K_4^{(i)}) \\ & -\exp(-K_s^{(i)}+K_\sigma^{(i)}-K_4^{(i)}) \\ & +\exp(-K_s^{(i)}-K_\sigma^{(i)}+K_4^{(i)}), \end{aligned} \tag{14}$$

and

$$\begin{aligned} q_4 = {}& \exp(K_s^{(i)}+K_\sigma^{(i)}+K_4^{(i)}) + \exp(K_s^{(i)}-K_\sigma^{(i)}-K_4^{(i)}) \\ & +\exp(-K_s^{(i)}+K_\sigma^{(i)}-K_4^{(i)}) \\ & +\exp(-K_s^{(i)}-K_\sigma^{(i)}+K_4^{(i)}), \end{aligned} \tag{15}$$

in which A_i is an additive constant associated with the ith decimation procedure and $K_s^{(i)}$, $K_\sigma^{(i)}$, and $K_4^{(i)}$ are the renormalized interaction parameters. From Eqs. (8)–(11), one can obtain that

$$\begin{aligned} A_i = {}& \frac{1}{4^m}(q_1^b+q_2^b+q_3^b+q_4^b)^{(m/4)}(q_1^b-q_2^b-q_3^b+q_4^b)^{(m/4)} \\ & \times(-q_1^b+q_2^b-q_3^b+q_4^b)^{(m/4)}(-q_1^b-q_2^b+q_3^b+q_4^b)^{(m/4)}, \end{aligned} \tag{16}$$

$$K_s^{(i-1)} = \frac{m}{4}\ln\frac{(q_1^b+q_2^b+q_3^b+q_4^b)(q_1^b-q_2^b-q_3^b+q_4^b)}{(-q_1^b+q_2^b-q_3^b+q_4^b)(-q_1^b-q_2^b+q_3^b+q_4^b)}, \tag{17}$$

$$K_\sigma^{(i-1)} = \frac{m}{4}\ln\frac{(q_1^b+q_2^b+q_3^b+q_4^b)(-q_1^b+q_2^b-q_3^b+q_4^b)}{(q_1^b-q_2^b-q_3^b+q_4^b)(-q_1^b-q_2^b+q_3^b+q_4^b)}, \tag{18}$$

and

$$K_4^{(i-1)} = \frac{m}{4}\ln\frac{(q_1^b+q_2^b+q_3^b+q_4^b)(-q_1^b-q_2^b+q_3^b+q_4^b)}{(q_1^b-q_2^b-q_3^b+q_4^b)(-q_1^b+q_2^b-q_3^b+q_4^b)}. \tag{19}$$

Equations (17)–(19) are the recursion relations of the renormalization-group transformation. If we consider, simultaneously, the term related to J_0 in Hamiltonian expression (1), then the recursion relations (17)–(19) of the renormalization-group transformation remain invariant in this case.

Furthermore, if we define three new parameters ω_1, ω_2, and ω_3 as

$$\omega_1 = \exp(-2K_\sigma-2K_4), \tag{20}$$

$$\omega_2 = \exp(-2K_s-2K_4), \tag{21}$$

and

$$\omega_3 = \exp(-2K_s-2K_\sigma), \tag{22}$$

then, from Eqs. (8)–(11), the following equations can be obtained:

$$\omega_1^{(i-1)} = \frac{(g_1^b-g_2^b-g_3^b+g_4^b)^m}{(g_1^b+g_2^b+g_3^b+g_4^b)^m}, \tag{23}$$

$$\omega_2^{(i-1)} = \frac{(-g_1^b+g_2^b-g_3^b+g_4^b)^m}{(g_1^b+g_2^b+g_3^b+g_4^b)^m}, \tag{24}$$

and

$$\omega_3^{(i-1)} = \frac{(-g_1^b-g_2^b+g_3^b+g_4^b)^m}{(g_1^b+g_2^b+g_3^b+g_4^b)^m}, \tag{25}$$

where

$$g_1 = 1+\omega_1^{(i)}-\omega_2^{(i)}-\omega_3^{(i)}, \tag{26}$$

$$g_2 = 1-\omega_1^{(i)}+\omega_2^{(i)}-\omega_3^{(i)}, \tag{27}$$

$$g_3 = 1-\omega_1^{(i)}-\omega_2^{(i)}+\omega_3^{(i)}, \tag{28}$$

and

$$g_4 = 1+\omega_1^{(i)}+\omega_2^{(i)}+\omega_3^{(i)}. \tag{29}$$

Equations (23)–(25) are a different version of the recursion relations, in the new parameter space $(\omega_1,\omega_2,\omega_3)$, of

TABLE I. Nontrivial fixed points with eigenvalues and critical exponents for $m=2$ and $b=2$.

Fixed point	$(\omega_1,\omega_2,\omega_3)$	$(\lambda_1,\lambda_2,\lambda_3)$	ν	ϕ
I_1	1,0.2956,0.2956	1.6786,0,0	1.3383	
I_2	0.2956,1,0.2956	1.6786,0,0	1.3383	
I_3	0.2956,0.2956,1	1.6786,0,0	1.3383	
U_1	0.2956,0,0	1.6786,0,0	1.3383	
U_2	0,0.2956,0	1.6786,0,0	1.3383	
U_3	0,0,0.2956	1.6786,0,0	1.3383	
V_1	0.2956,0.2956,0.08738	1.6786,1.6786,0.7044	1.3383	1
V_2	0.2956,0.08738,0.2956	1.6786,1.6786,0.7044	1.3383	1
V_3	0.08738,0.2956,0.2956	1.6786,1.6786,0.7044	1.3383	1
Potts	0.2203,0.2203,0.2203	1.8526,1.2778,1.2778	1.1242	0.3976

the renormalization-group transformation. For simplicity and convenience hereafter we shall investigate fixed points, critical exponents, and phase diagram in this space and restrict ourselves to the ferromagnetic case, i.e., $0\leqslant\omega_1,\omega_2,\omega_3\leqslant 1$.

III. FIXED POINTS AND PHASE DIAGRAMS

The recursion relations (23)–(25) of the renormalization-group transformation will produce all fixed points and result in the phase diagram for the anisotropic AT model on the family of the diamond-type hierarchical lattices for any given m and b. There are fifteen fixed points in total, including five trivial (completely stable) fixed points and ten nontrivial fixed points. As presented in Table I, these ten nontrivial fixed points can be divided into four sets according to their locations in the parameter space $(\omega_1,\omega_2,\omega_3)$. The first set I_k contains three fixed points at $(\omega_I,\omega_I,1)$, $(\omega_I,1,\omega_I)$, and $(1,\omega_I,\omega_I)$, all of which are associated with only one relevant eigenvalue of the renormalization-group transformation matrix; the second set U_k includes three fixed points at $(\omega_I,0,0)$, $(0,\omega_I,0)$, and $(0,0,\omega_I)$, all of which are related to one relevant eigenvalue as well; the third V_k consists of three fixed points at $(\omega_I,\omega_I,\omega_I^2)$, $(\omega_I,\omega_I^2,\omega_I)$, and $(\omega_I^2,\omega_I,\omega_I)$, all of which are connected with two equal relevant eigenvalues; the fourth only contains one fixed point, i.e., the *Potts* fixed point, at $(\omega_P,\omega_P,\omega_P)$, which is associated with three relevant eigenvalues. We present as examples, two phase diagrams, i.e., Figs. 2 and 3, for the anisotropic AT model on the family of the diamond-type hierarchical lattices, which correspond to the cases of $m=2$, $b=2$, and $m=3$, $b=2$, respectively. Both of them indicate that the phase diagram consists of five phases, i.e., (a) the fully disordered paramagnetic phase P, in which $\langle s\rangle=0$, $\langle\sigma\rangle=0$, and $\langle s\sigma\rangle=0$; (b) the fully ordered ferromagnetic phase F, in which $\langle s\rangle\neq 0$, $\langle\sigma\rangle\neq 0$, and $\langle s\sigma\rangle\neq 0$; (c) the partially ordered ferromagnetic phase F_s, in which $\langle s\rangle\neq 0$, $\langle\sigma\rangle=0$, and $\langle s\sigma\rangle=0$; (d) the partially ordered ferromagnetic phase F_σ, in which $\langle\sigma\rangle\neq 0$, $\langle s\rangle=0$, and $\langle s\sigma\rangle=0$; and (e) the partially ordered ferromagnetic phase $F_{s\sigma}$, in which $\langle s\sigma\rangle\neq 0$, $\langle s\rangle=0$, and $\langle\sigma\rangle=0$. The three-dimensional domains of attraction of these five trivial fixed points, located at (0,0,0), (1,1,1), (1,0,0), (0,1,0), and (0,0,1), correspond to five phases F, P, F_s, F_σ, and $F_{s\sigma}$, respectively. Three two-dimensional critical surfaces, corresponding to the domains of attraction of the three singly unstable fixed points of the set U_k, respectively, constitute the boundaries of the phase F. In the meantime, the boundaries of the phase P is composed of the other three two-dimensional critical surfaces, corresponding to the domains of attraction of the three singly unstable fixed points of the set I_k, respectively. These two-dimensional critical surfaces join along three lines, corresponding to the domains of attraction of the three doubly unstable fixed points of the set V_k, respectively. The three lines meet at the completely unstable fixed point, i.e., the Potts fixed point, located at $(\omega_P,\omega_P,\omega_P)$. At this point, the anisotropic AT model has the symmetry of a four-state Potts model.

It is essential to point out that both ω_I and ω_P are dependent on the values of m and b. As presented in Figs. 4 and 5, for a given b, both ω_I and ω_P increase monotonically as m

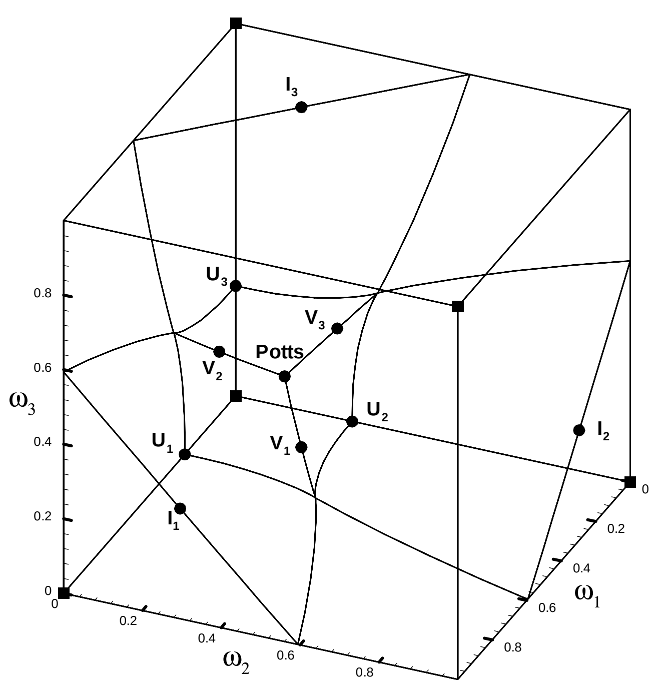

FIG. 2. Phase diagram for the anisotropic Ashkin-Teller model on the family of the diamond-type hierarchical lattices for $b=2$ and $m=2$, where $\omega_I=0.2956$, $\omega_P=0.2203$, and the symbol ■ denotes the five trivial fixed points.

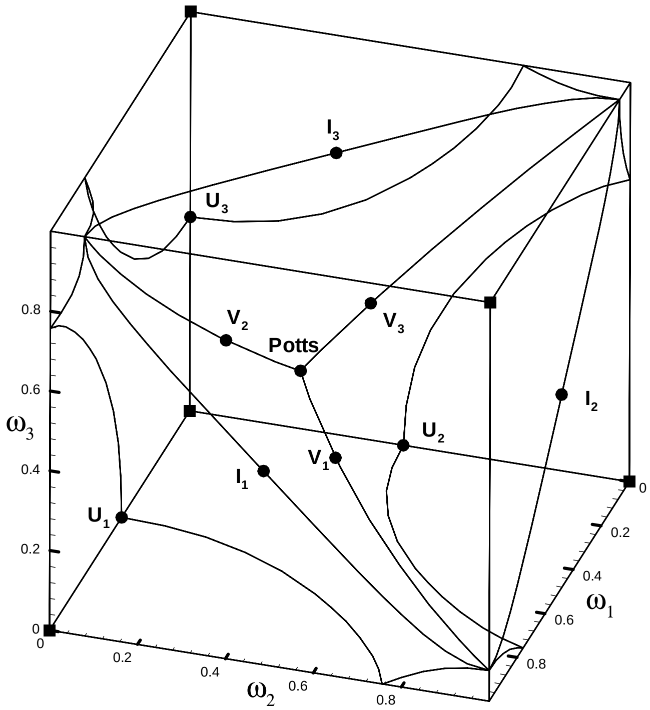

FIG. 3. Phase diagram for the anisotropic Ashkin-Teller model on the family of the diamond-type hierarchical lattices for $b=2$ and $m=3$, where $\omega_I=0.4859$, $\omega_P=0.3689$, and the symbol ■ denotes the five trivial fixed points.

increases. When m becomes large, the curves may attain plateaux at well-defined values. But, for a given m, both ω_I and ω_P decrease monotonically as b increases. When b becomes large, the curves may also reach the stable levels at well-defined values. Thus, for different sets of m and b, one can obtain different sets of fixed points and different phase diagrams. As shown in Figs. 2 and 3, the phase diagram for the anisotropic AT model on the family of the diamond-type hierarchical lattices possesses very rich variations.

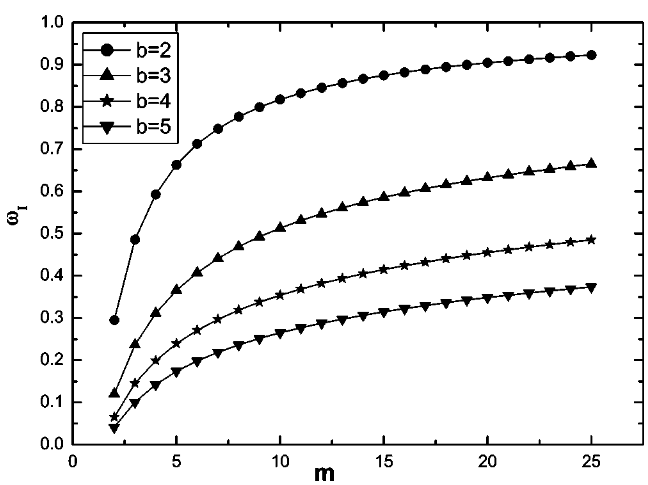

FIG. 4. Dependence of one of the coordinates, ω_I, of the nontrivial fixed points on the number of branches m, and the number of bonds per branch b of the generator of the family of the diamond-type hierarchical lattices.

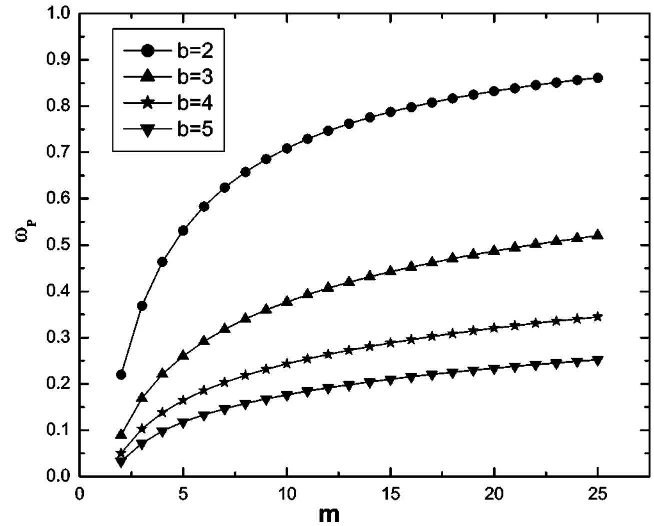

FIG. 5. Dependence of one of the coordinates, ω_P, of the Potts fixed point on the number of branches m, and the number of bonds per branch b of the generator of the family of the diamond-type hierarchical lattices.

In general, the above results that the phase diagram for the anisotropic AT model on the family of the diamond-type hierarchical lattices consists of five phases and fifteen fixed points are consistent with those of Refs. [17,18], where the anisotropic AT model on the square lattice has been investigated, as well as with those obtained by Bezerra *et al.* [26] in the investigations of the anisotropic AT model on a kind of self-dual hierarchical lattice. However, in the phase diagram for the case of $d_f=3$, e.g., $b=2$ and $m=4$, we cannot produce the first-order transition line(s), which can be found in Refs. [15,19], concerning the AT model in three dimensions. With regard to the locations of the nontrivial fixed points, it can be found that $\omega_I=1/(1+\sqrt{2})$, $\omega_P=1/(1+\sqrt{4})$ in Ref. [17], $\omega_I=0.422$, $\omega_P=0.341$ in Ref. [18], and $\omega_I=\sqrt{2}-1$, $\omega_P=1/3$ in Ref. [26]. Because of the dependence of ω_I and ω_P on the parameters m and b of the hierarchical lattices, we only take the case of $b=2$ as an example. In this case (see Figs. 4 and 5), $\omega_I=0.2956$, $\omega_P=0.2203$ when $m=2$, i.e., $d_f=2$; $\omega_I=0.4859$, $\omega_P=0.3689$ when $m=3$; $\omega_I=0.5933$, $\omega_P=0.4638$ when $m=4$. Therefore, one can find that the results of ω_I and ω_P for the case of $b=2$ and $m=3$ are comparatively close to those already known in Refs. [17,18,26].

IV. CRITICAL EXPONENTS

Using the recursion relations (23)–(25) of the renormalization-group transformation, one can calculate the correlation length critical exponent ν and the crossover exponent ϕ from the scaling factor b and the relevant eigenvalues for any given m and b [29–31]. It can be found that two sets I_k and U_k of the nontrivial fixed points are in the same case as the single identical relevant eigenvalue, thus all of them have the same correlation length critical exponent ν as the Ising universality class [27]. Having two equal relevant eigenvalues identical with that of the former two sets

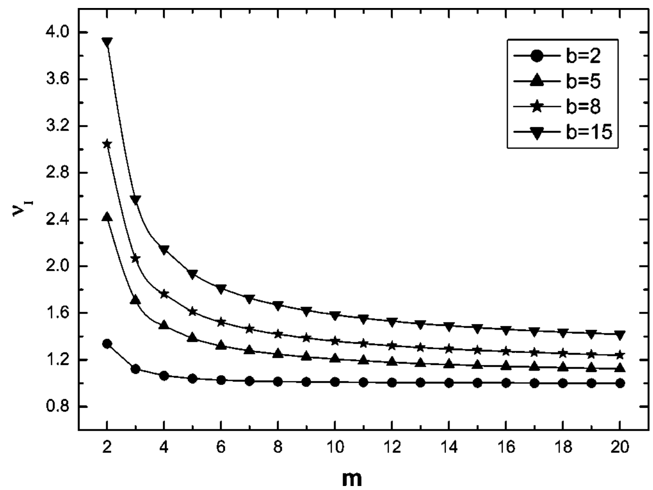

FIG. 6. Variations of the correlation length critical exponent ν_I with the number of branches m, and the number of bonds per branch b of the generator of the family of the diamond-type hierarchical lattices.

I_k and U_k, the set V_k of the nontrivial fixed points are associated with the same correlation length critical exponent ν as well as the only one crossover exponent ϕ equal to 1. As far as the Potts fixed point is concerned, it is related to three relevant eigenvalues, among which the two smaller ones are identical with each other, hence it possesses the correlation length critical exponent ν which is identical with that of the four-state Potts model on the same lattice, as well as two equal crossover exponents ϕ. As an example, the results in the case of $b=2$ and $m=2$ are presented in Table I.

It is interesting to investigate the variations of the critical exponents ν and ϕ with b, m, and d_f, which may be helpful to the discussion about the universality class. For the sake of convenience, let ν_P and ϕ_P denote the correlation length critical exponent and the crossover exponent associated with the Potts fixed point, respectively, and ν_I represent the correlation length critical exponent associated with the other

TABLE II. Different critical exponents for the same fractal dimension d_f but different m and b, and the invariance of the crossover exponent ϕ_P under the interchange of the values of m and b.

	$d_f=1.5$			$d_f=3$		
m	2	3	4	4	9	16
b	4	9	16	2	3	4
ν_p	1.8337	1.8749	1.9135	0.9168	0.9374	0.9567
ν_I	2.1296	2.1597	2.1886	1.0648	1.0799	1.0943
ϕ_p	0.5054	0.5133	0.5206	0.5054	0.5133	0.5206

nontrivial fixed points. As shown in Fig. 6, for a given b, ν_I decreases monotonically as m increases. One can observe a convergence towards saturation values when m becomes large. However, for a given m, ν_I increases monotonically as b increases. With d_f increasing, ν_I decreases monotonically, but ν_I is not completely decided by d_f, ν_I has some difference for the same d_f but different b or m (see Fig. 7 and Table II). As presented in Fig. 8, for a given b, ν_P decreases monotonically as m increases, but there is an exception for $m\geqslant 7$ when $b=2$. Also, one can observe a convergence towards saturation values when m becomes large. For a given m, ν_P increases monotonically as b increases, but there is also an exception for $b=2$ when $m\geqslant 12$. With d_f increasing, ν_P decreases monotonically except for the case of $b=2$, but ν_P is not fully determined by d_f, ν_P has some difference for the same d_f but different b or m (see Fig. 9 and Table II). As shown in Fig. 10, for a given b (m), with m (b) increasing, ϕ_P decreases first, reaches a minimum at $m\leqslant b$ $(b\leqslant m)$, and then increases except for the case when $b=2$ $(m=2)$ in which case ϕ_P increases monotonically. We also find that ϕ_P is invariant under the interchange of the values of m and b (see Table II). For a given b (m), with d_f increasing (decreasing), ϕ_P decreases first, comes to a minimum, and then increases except for the case when $b=2$ $(m=2)$ in which

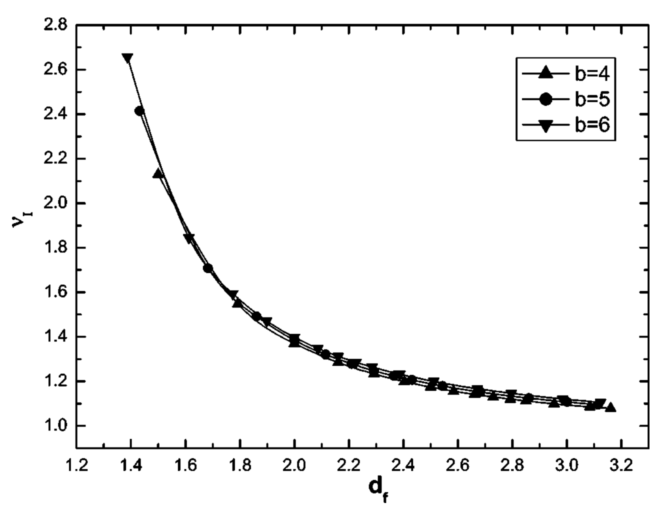

FIG. 7. The correlation length critical exponent ν_I vs the fractal dimension d_f of the family of the diamond-type hierarchical lattices.

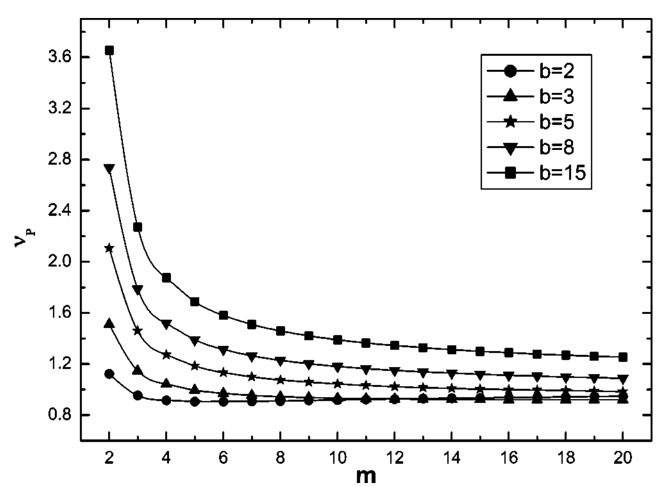

FIG. 8. Variations of the correlation length critical exponent ν_P with the number of branches m, and the number of bonds per branch b of the generator of the family of the diamond-type hierarchical lattices.

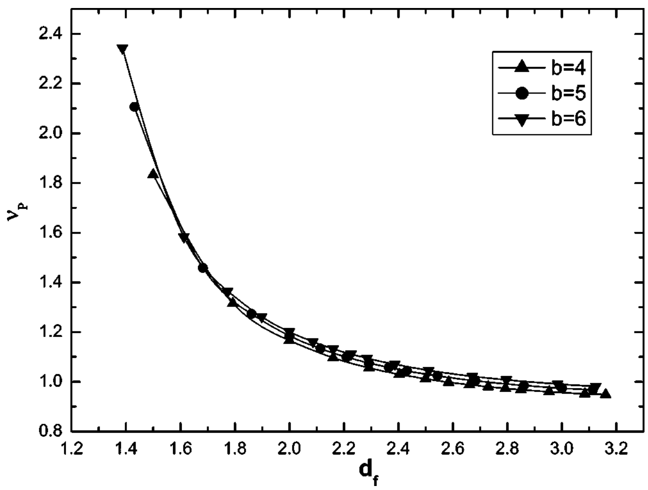

FIG. 9. The correlation length critical exponent ν_P vs the fractal dimension d_f of the family of the diamond-type hierarchical lattices.

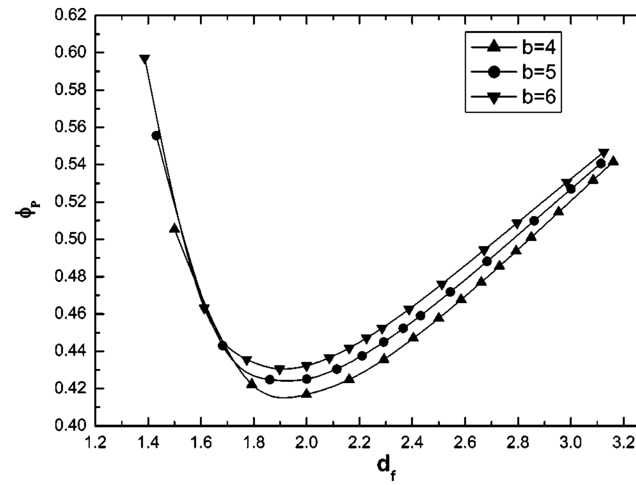

FIG. 11. The crossover critical exponent ϕ_P vs the fractal dimension d_f of the family of the diamond-type hierarchical lattices.

ϕ_P increases monotonically. But ϕ_P is not completely decided by d_f, ϕ_P has some difference in the case of the same d_f but different b or m (see Fig. 11 and Table II). It can be concluded from the above investigations that the critical exponents (the correlation length critical exponent ν and the crossover exponent ϕ) for the anisotropic AT model on the family of the diamond-type hierarchical lattices not only depend on the fractal dimension d_f but also the concrete geometrical parameters, i.e., b and m, of the lattices.

For the square lattice, the exact values of the correlation length critical exponent are $\nu_I = 1$ and $\nu_P = 2/3$ for the Ising and Potts universality class, respectively [14]. In addition, for a kind of self-dual hierarchical lattice, Bezerra *et al.* [26] have obtained that $\nu_I = 1.149$ and $\nu_P = 0.948$. Due to reasons that both ν_I and ν_P are dependent on the parameters m and b of the hierarchical lattices, we only take the case of $b=2$ as an example. In this case (see Figs. 6 and 8), $\nu_I = 1.3383$, $\nu_P = 1.1242$ when $m=2$, i.e., $d_f = 2$; $\nu_I = 1.1227$, $\nu_P = 0.9534$ when $m=3$; ...; $\nu_I = 1.0276$, $\nu_P = 0.9062$ when $m=6$; $\nu_I = 1.0201$, $\nu_P = 0.9083$ when $m=7$. Therefore, one can find that the results of ν_I and ν_P for the cases of $b=2$, $m=6$ and $b=2, m=3$ are comparatively close to those of Ref. [14] and Ref. [26], respectively.

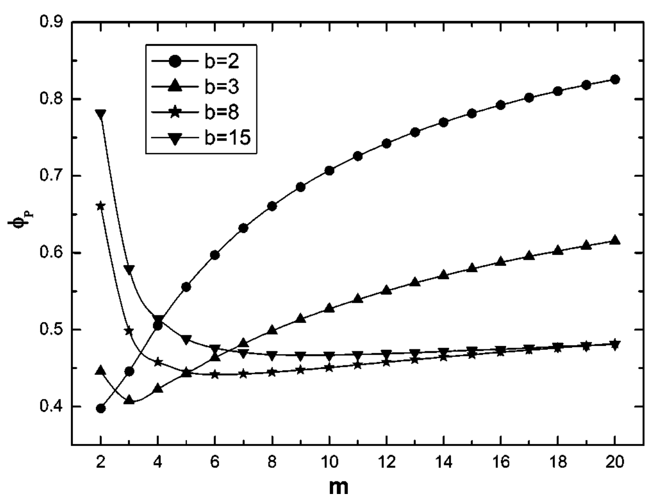

FIG. 10. Variations of the crossover critical exponent ϕ_P with the number of branches m, and the number of bonds per branch b of the generator of the family of the diamond-type hierarchical lattices.

V. CONCLUSION AND DISCUSSION

In this paper, by means of the transfer-matrix method and the real-space renormalization-group transformation, we study the phase transitions of the anisotropic Ashkin-Teller model on a family of diamond-type hierarchical lattices. It can be found that for different sets of m and b, the phase diagram for the ferromagnetic case consists of five phases, i.e., the fully disordered paramagnetic phase P, the fully ordered ferromagnetic phase F, and three partially ordered ferromagnetic phases F_s, F_σ, and $F_{s\sigma}$, as well as ten nontrivial fixed points. The correlation length critical exponents and the crossover exponents are also calculated. In addition, as we know, universality is one of the three pillars of modern critical phenomena [32], and it depends on a number of factors. On a Bravais lattice, the universality criteria are dimensionality and symmetry. However, through the investigations of the variations of the critical exponents with the fractal dimension d_f, the number of branches m, as well as the number of bonds per branch b of the generator of the hierarchical lattices, we have shown the difficulties in searching for the complete set of universality criteria on a hierarchical lattice. This problem deserves further attention.

ACKNOWLEDGMENTS

J.-X.L. would like to thank Dr. W. A. Guo and Dr. X. M. Kong for their valuable discussions. This work was supported by the National Natural Science Foundation of China under Grant No. 10175008.

[1] J. Ashkin and E. Teller, Phys. Rev. **64**, 178 (1944).
[2] C. Fan, Phys. Lett. **39A**, 136 (1972).
[3] F.J. Wegner, J. Phys. C **5**, L131 (1972).
[4] P. Bak, P. Kleban, W.N. Unertl, J. Ochab, G. Akinci, N.C. Bartelt, and T.L. Einstein, Phys. Rev. Lett. **54**, 1539 (1985).
[5] J. Chahine, J.R. Drugowich de Felício, and N. Caticha, J. Phys. A **22**, 1639 (1989).
[6] S. Wiseman and E. Domany, Phys. Rev. E **48**, 4080 (1993).
[7] S. Wiseman and E. Domany, Phys. Rev. E **51**, 3074 (1995).
[8] G. Kamieniarz, P. Kozlowski, and R. Dekeyser, Phys. Rev. E **55**, 3724 (1997).
[9] L.P. Kadanoff, Phys. Rev. Lett. **39**, 903 (1977).
[10] H.J.F. Knops, Ann. Phys. (N.Y.) **128**, 448 (1980).
[11] M.P.M. den Nijs, Phys. Rev. B **23**, 6111 (1981).
[12] A.M. Mariz, C. Tsallis, and P. Fulco, Phys. Rev. B **32**, 6055 (1985).
[13] J.A. Plascak and F.C. Sá Barreto, J. Phys. A **19**, 2195 (1986).
[14] R.J. Baxter, *Exactly Solved Models in Statistical Mechanics* (Academic, New York, 1982).
[15] R.V. Ditzian, J.R. Banavar, G.S. Grest, and L.P. Kadanoff, Phys. Rev. B **22**, 2542 (1980).
[16] F.Y. Wu and K.Y. Lin, J. Phys. C **7**, L181 (1974).
[17] E. Domany and E.K. Riedel, Phys. Rev. B **19**, 5817 (1979).
[18] M. Badehdah, S. Bekhechi, A. Benyoussef, and M. Touzani, Physica B **291**, 394 (2000).
[19] S. Bekhechi, A. Benyoussef, A. Elkenz, B. Ettaki, and M. Loulidi, Physica A **264**, 503 (1999).
[20] A.N. Berker and S. Ostlund, J. Phys. C **12**, 4961 (1979).
[21] M. Kaufman and R.B. Griffiths, Phys. Rev. B **24**, 496 (1981).
[22] A. Efrat and M. Schwartz, Phys. Rev. E **63**, 036124 (2001).
[23] A. Efrat, Phys. Rev. E **63**, 066112 (2001).
[24] F.D. Nobre and E.M.F. Curado, Phys. Rev. E **66**, 036107 (2002).
[25] J. Török, S. Krishnamurthy, J. Kertész, and S. Roux, Phys. Rev. E **67**, 026108 (2003).
[26] C.G. Bezerra, A.M. Mariz, J.M. de Araújo, and F.A. da Costa, Physica A **292**, 429 (2001).
[27] Z.R. Yang, Phys. Rev. B **38**, 728 (1988).
[28] Y. Qin and Z.R. Yang, Phys. Rev. B **43**, 8576 (1991).
[29] J.R. Melrose, J. Phys. A **16**, 3077 (1983).
[30] B. Hu, Phys. Rev. Lett. **55**, 2316 (1985).
[31] C. Tsallis and A.C.N. de Magalhães, Phys. Rep. **268**, 305 (1996).
[32] H.E. Stanley, Rev. Mod. Phys. **71**, S358 (1999).